

DEEP SELF-BURIAL OF RADIOACTIVE WASTES BY ROCK-MELTING CAPSULES

RADIOACTIVE WASTE

STANLEY E. LOGAN *University of New Mexico*
Chemical and Nuclear Engineering Department, Albuquerque, New Mexico 87106

KEYWORDS: *rocks, melting, radioactive wastes, underground disposal, heating, solidification, depth, radioactive waste disposal*

Received July 2, 1973
Revised October 22, 1973

The rock-melting-capsule concept utilizes decay heat from high-level radioactive wastes in a container to melt rock. Descent by gravity achieves deep disposal. Molten rock resolidifies in the wake of the capsule, providing permanent isolation from the environment.

Results calculated for:

- 1. waste categories of fission products, actinides, and Sr + Cs*
- 2. spherical capsule radii of 25, 50, and 100 cm*
- 3. waste oxide volume fractions of 0.15, 0.30, and 0.50*
- 4. basalt and granite rock types*

indicate adequate heat generation for rock melting, maximum depth increases with capsule size and waste concentration, with depths greater than 10 km obtainable by each waste category.

Further work is recommended to investigate corrosion and erosion of refractory container materials in contact with waste oxide melts and molten rock.

Lewis, and Braun¹ have proposed the Plowshare concept, which holds considerable promise, in which liquid wastes would be injected into a deep nuclear chimney where they ultimately produce rock melting and where the wastes become incorporated in the molten rock which subsequently resolidifies. Another method, proposed here, may permit placing wastes at a greater depth with an almost immediate and permanent isolation from the surface environment: This is the rock-melting-capsule concept, utilizing the decay heat from waste capsules to melt rock and descend by gravity for self-burial. Parallel analytical work on self-burying waste capsules in salt domes and granite has recently been done in Europe by Donea, Giuliani, and Kestemont.² An analytical study of the self-burial of a radioisotope space power heat source following reentry and earth impact has been reported by Easton.³

ROCK-MELTING-CAPSULE CONCEPT

A drilled and partially or fully cased hole up to 2 km deep is established to permit the release of a waste capsule and the start of rock melt at a safe depth. The waste-filled container, with a temporary separable cooling system attached, is lowered to the bottom of the hole (Fig. 1). Remote preparation for release includes adding a startup thermal contact medium such as granular aluminum, which flows into the space between the capsule and rock walls, plus, if necessary, a temporary seal layer of material such as concrete. The cooling system is then shut down and retrieved for reuse. In the absence of cooling, the waste contents heat up and melt, the capsule surface temperature rises, and the thermal contact medium melts, followed by the start of rock melt and capsule descent (Fig. 2). The molten rock

INTRODUCTION

Management of high-level radioactive wastes from the reprocessing of nuclear fuel is becoming a more significant problem as the number of nuclear power plants increases. There is a need for permanent disposal methods which do not subject future generations to a risk from radioactive residues, require continuing surveillance, or result in loss of land for other uses. Cohen,

wake resolidifies, forming a permanent seal. After a suitable delay, the bottom of the hole is prepared to receive the next capsule, thus permitting many capsules to be released from the same hole.

The container serves as a separator between the waste contents and molten rock. As such, it is not required to maintain a rigid structural shape once cooling is terminated and descent begins. Lithostatic pressure increases at a rate of ~ 0.3 kbar per kilometer of depth (1 kbar = 14 500 psi). This will produce a gradual compression of the capsule. Assuming that the bulk modulus of the waste material is no greater than that of the surrounding rock, the density differential required for descent will be maintained. Initial velocity is less than a few meters per day, but descent may continue for many years and attain great depths, depending on the corrosion life of the container

and the radioactive decay characteristics of the waste. Determination of a suitable container material, along with a possible need for chemical adjustment of the waste to obtain adequate corrosion life with a reasonable wall thickness, is a difficult problem requiring additional investigation.

The basement rock underlying upper sedimentary layers is a crystalline silicate rock, either basalt or granite. This study investigates descent through both of these rock types. The thick sequence of basalt existing as flow layers in the Columbia Plateau has been extensively studied for waste storage suitability.⁴

ANALYSIS

The model for analytic development is shown in Fig. 3. A spherical shape of the waste capsule is assumed with outside radius a and container wall thickness s . The local bulk temperature of the rock, T_r , increases with depth in accordance with the geologic temperature gradient. This gradient varies considerably with location but a typical value of $20^\circ\text{C}/\text{km}$ is used here; 10°C at the surface is assumed. The heat generation rate q''' depends on the radioactive isotopes present, their concentration, and the age of the waste; this is discussed later. The surface temperature of the sphere, T_c , is assumed to be uniform in the model. When the sphere temperature exceeds the melting temperature of the surrounding rock, formation of a rock-melt layer occurs; with the capsule density

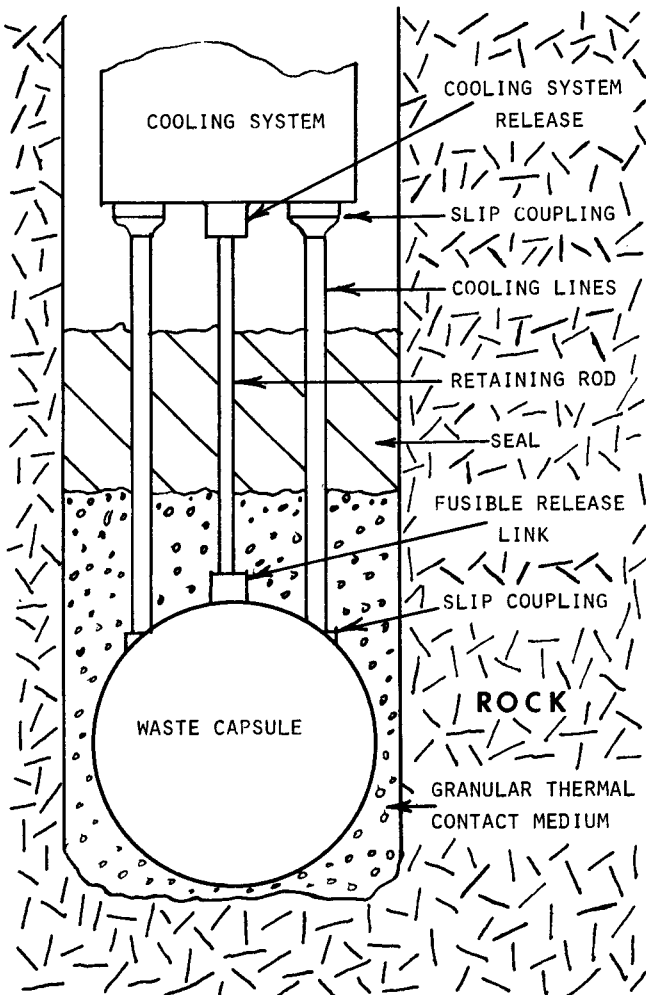


Fig. 1. Waste capsule with temporary cooling system. Ready for release.

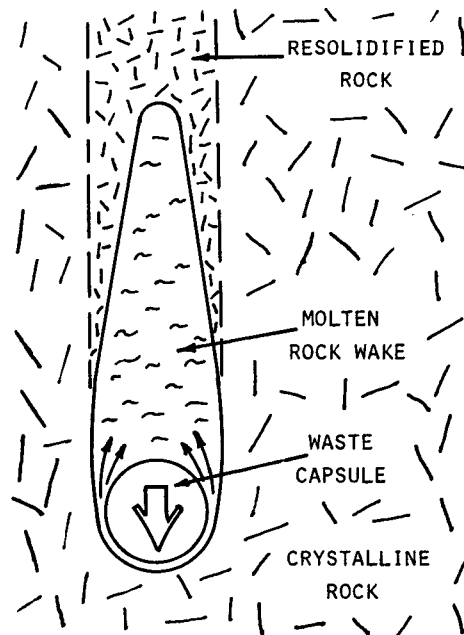


Fig. 2. Descending waste capsule.

greater than the rock density, the capsule settles and displaces the melt in a continuing process. The velocity of descent is then determined by the rate of energy exchange with the rock underneath and by hydrodynamic limitations associated with rock-melt displacement.

Energy Criteria for Determining Descent Velocity

The energy required per unit volume of rock to raise the temperature from local ambient, through the melting range, to the surface temperature of the capsule is

$$h_m = (T_c - T_r)\rho c + h_f\rho, \quad \text{cal/cm}^3, \quad (1)$$

where

T_c = capsule surface temperature, °K

T_r = ambient rock temperature, °K

ρ = rock density, g/cm³

c = rock specific heat, cal/(g deg)

h_f = rock heat of fusion, cal/g.

The energy rate for rock melting with descent velocity v_e and capsule radius a is

$$q_m = \pi a^2 h_m v_e, \quad \text{cal/sec} \quad (2)$$

The total heat generation rate by the high-level waste material is

$$q_w = q''' \frac{4}{3} \pi (a - s)^3, \quad \text{cal/sec} \quad (3)$$

where

q''' = volume heat generation rate, cal/(sec cm³)

s = wall thickness of capsule shell, cm.

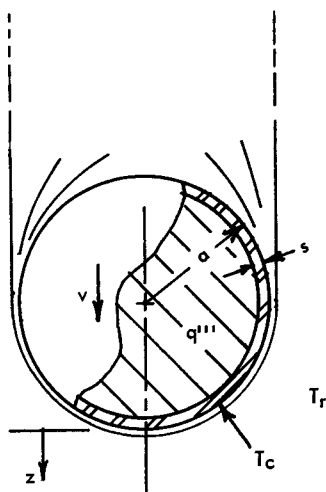


Fig. 3. Analytic model.

A portion of the capsule heat is lost laterally. By letting b denote the fraction of heat directed downward for rock melting, the energy balance becomes

$$bq_w = q_m \quad ; \quad (4)$$

then, velocity by the energy criteria becomes

$$v = \frac{1.33 b q''' (a - s)^3}{a^2 h} \quad (5)$$

A simplified model was set up to evaluate the heat fraction b . A cylinder of the same radius and surface area as the sphere was considered (Fig. 4), with uniform conduction heat loss per unit area, q_c'' , and superimposed rock-melt heat per unit area in the direction of motion, q_m'' . The value of b is the ratio of the downward component sum to the total heat transfer, or

$$b = \frac{\pi a^2 q_c'' + \pi a^2 q_m''}{4\pi a^2 q_c'' + \pi a^2 q_m''} = \frac{q_c'' + q_m''}{4q_c'' + q_m''} \quad (6)$$

The surface heat transfer rate for a stationary sphere at steady state is

$$q'' = \lambda \left(\frac{T_c - T_r}{a} \right), \quad \text{cal}/(\text{sec cm}^2) \quad (7)$$

where λ is the rock thermal conductivity, cal/(cm sec deg).

A moving sphere develops a larger temperature gradient than the steady-state value. Using temperature response charts⁵ and an average time of exposure to the moving heat source equal to $a/2v$, an empirical relation for the moving source heat transfer rate, evaluated for the cylindrical surface of the model, modifies Eq. (7) to become

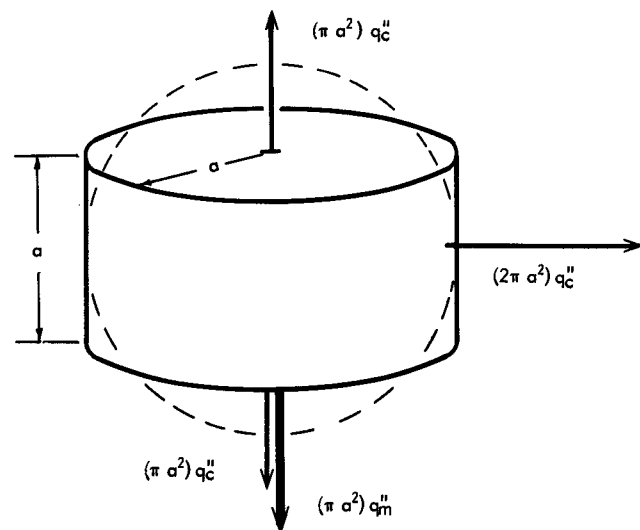


Fig. 4. Moving heat source model for rock-melting heat fraction.

$$q_c'' = \lambda \left(\frac{T_c - T_r}{a} \right) \left(\frac{2av}{\alpha} \right)^{0.382}, \text{ cal}/(\text{sec cm}^2), \quad (8)$$

where $\alpha = \lambda/\rho c$, thermal diffusivity, cm^2/sec .

While the modification factor does not hold at zero velocity, it approaches unity as velocity decreases to a few centimeters per day. The rock-melt heat transfer rate is simply

$$q_m'' = v h_m, \text{ cal}/(\text{sec cm}^2). \quad (9)$$

The low thermal conductivity of rock effectively insulates the moving capsule from appreciable lateral heat loss, providing a value for b of ~ 0.8 for a velocity of 3 m/day. As zero velocity is approached, the proportion represented by the lateral loss increases and the downward heat fraction approaches the ratio of projected area to total sphere area, or 0.25.

As decay of the waste material proceeds, q''' and v_e decrease until a threshold value of heat generation rate is reached. This is considered to be the value of q''' for which the surface temperature of an at-rest sphere is equal to the melting temperature of the rock at equilibrium; that is,

$$q_{th}''' = \frac{3\lambda}{a^2} (T_m - T_r), \text{ cal}/(\text{sec cm}^3), \quad (10)$$

where T_m is the melting temperature of rock, $^\circ\text{K}$.

Hydrodynamic Criteria for Determining Descent Velocity

Molten rock, formed in a thin layer around the descending capsule, flows through the film-like channel created between solid rock and the capsule surface. Studies of rock-melting drills at the Los Alamos Scientific Laboratory (LASL)^{6,7} provide an analysis of the flow of molten rock around a hot penetrator. Considering the penetrator to stand still and the rock to move upward with a bulk velocity v , the problem becomes one of hydrodynamic flow around a hot barrier. Rock in contact with the hot surface approaches the surface temperature, T_c . "Upstream" (z direction), the temperature excess over the ambient rock temperature decays exponentially with distance z as

$$(T - T_r) = (T_c - T_r) \exp\left(-\frac{v}{\alpha} z\right), \text{ } ^\circ\text{C}. \quad (11)$$

Viscosity is very sensitive to temperature, varying with the form $\eta = A \exp(E/RT)$, where E is the activation energy (cal/mol) (discussed later in the section on rock properties) and R is the gas constant [1.987 cal/(deg mol)]. The viscosity variation with z may be represented by

$$\eta = \eta_c \exp(\beta z), \quad (12)$$

where

$$\beta = \frac{Ev}{RT_c \alpha} \left(\frac{T_c - T_r}{T_c} \right), \text{ cm}^{-1} \quad (13)$$

$\eta_c =$ viscosity at T_c , P .

Armstrong et al.⁶ present the Navier-Stokes equation for radial and axial pressure gradients for a cylindrical system with varying viscosity and, using the continuity equation $\nabla \cdot v = 0$, obtain a solution for pressure as a function of radial position r . Robinson et al.⁷ extend the solution to apply to a conical penetrator of included half-angle θ , and obtain

$$p = \frac{1}{4} \eta_c \beta v \sin^2 \theta (a^2 - r^2), \text{ dyne}/\text{cm}^2. \quad (14)$$

By considering a penetrator with $\theta = \pi/4$ (90 deg included angle), integrating for total force from $r = 0$ to $r = a$, and dividing by the projected area of the penetrator, the average pressure becomes

$$\bar{p} = 0.062 \eta_c \beta^3 v a^2, \text{ dyne}/\text{cm}^2. \quad (15)$$

By approximating a hemisphere with a series of conical sections, the LASL solution may be extended to apply to a spherical penetrator. This results in an increase in the value of the coefficient, obtaining for the average pressure from displacement of rock melt (resisting capsule descent),

$$\bar{p} = 0.083 \eta_c \beta^3 v a^2, \text{ dyne}/\text{cm}^2. \quad (16)$$

In equilibrium, this average pressure must be equal to the net buoyant force per unit projected area,

$$\bar{p} = \left(\frac{4}{3}\right) (980.6) a (\rho_c - \rho), \text{ dyne}/\text{cm}^2, \quad (17)$$

where

$\rho_c =$ average capsule density, g/cm^3

980.6 = acceleration due to gravity, cm/sec^2 .

Average capsule density is obtained by including the mass of the container as well as the waste contents. Substituting for β from Eq. (13) in Eq. (16) and solving for v , the hydrodynamically limited velocity, v_h , is obtained:

$$v_h = \left\{ \bar{p}/0.083 \eta_c a^2 \left[\frac{E}{RT_c \alpha} \left(\frac{T_c - T_r}{T_c} \right) \right]^3 \right\}^{0.25}, \text{ cm}/\text{sec}, \quad (18)$$

in which \bar{p} is obtained from Eq. (17).

Within limits, capsule surface temperature, T_c , adjusts such that $v_h \rightarrow v_e$.

HIGH-LEVEL RADIOACTIVE WASTE

Wastes generated by the reprocessing of spent fuel include fission products and actinides (trans-

uranium elements). Almost all of the fission products appear in the high-level waste stream with trace amounts going to several categories of low-level waste. Actinide concentrations depend on recovery efficiency, and they are found in the high-level, low-level, and cladding wastes. Oak Ridge National Laboratory tabulations of the masses, radioactivity, and thermal power of significant fission product and actinide isotopes in wastes for a reference light water reactor⁸ are used here. An enrichment of 3.3% and a burnup to 33 000 MWd/MT at an average specific power of 30 MW/MT are assumed.

Table I lists the total mass of each waste category per 10³ MWd(th). The masses, after conversion to oxides by calcining (but not including added inert materials), and the calculated oxide densities are also listed. Recovery is assumed to be 99.5% for uranium and plutonium and 70% for neptunium. Americium, curium, and small amounts of thorium and protactinium are included as waste. After a waste age of 10 yr, most of the fission product activity is due to ⁹⁰Sr and ¹³⁷Cs and their short half-life daughters ⁹⁰Y and ^{137m}Ba, respectively. A waste category of Sr + Cs is therefore included to permit studying possible benefits from isolation and separate disposal of these elements. While the actinides tend to be dispersed through several categories of waste, it is assumed here for study purposes that they are isolated and collected as a separate group. The economic feasibility of various degrees of actinide isolation is subject to further study.

TABLE I
Masses and Densities of Pure Wastes from Reprocessing LWR Spent Fuel

Waste Type	Fission Products	Actinides	Sr + Cs
Total mass [g/10 ³ MWd(th)]	887	159	109
Oxide mass increase factor	1.21	1.13	1.09
Oxide mass [g/10 ³ MWd(th)]	1075	179	119
Oxide density (g/cm ³)	6.34	10.9	4.47

TABLE II
Volume Heat Generation Rate, q''' , for Waste Oxides [cal/(sec cm³)]

Age (yr)	Fission Products	Actinides	Sr + Cs
0.41	0.824	0.284	1.000
1	0.427	0.139	0.795
10	0.439×10^{-1}	0.311×10^{-1}	0.261
100	0.444×10^{-2}	0.442×10^{-2}	0.278×10^{-1}
1000	0.755×10^{-6}	0.100×10^{-2}	0.171×10^{-10}

The volume heat generation rates for pure waste oxides are given in Table II and plotted in Fig. 5 as a function of time. A single radioactive isotope or a mixture of more than one isotope having close to the same half-lives decay exponentially as $\exp(-0.693 t/t_h)$, but a mixture of isotopes having a range of half-lives decays according to the relation $A_2/A_1 = (t_2/t_1)^{-k}$. This last expression best describes the decay of heat generation rate for actinides over the full range of ages and for fission products and Sr + Cs up to an age of 10 yr. Beyond 10 yr, both of the fission product categories are dominated by the isotopes ⁹⁰Sr and ¹³⁷Cs (half-lives of 27.7 and 30.0 yr, respectively) and the first exponential variation applies.

Initially, high-level wastes are primarily aqueous solutions of inorganic nitrate salts, including nonradioactive salts added during fuel reprocessing.⁸ Processes for solidifying this waste add melt-making fluxes such as phosphates, borophosphates, silicates, borosilicates, and borates. High temperatures during solidification dehydrate the mixture, decompose the nitrates, and form oxides. A process yielding a glass product provides the density needed for the disposal capsule concept discussed here. Granular or powder forms have insufficient density. It is convenient to place waste quantities on a volume basis for capsule evaluations. Accordingly, Table III lists the density and annual volumes of waste

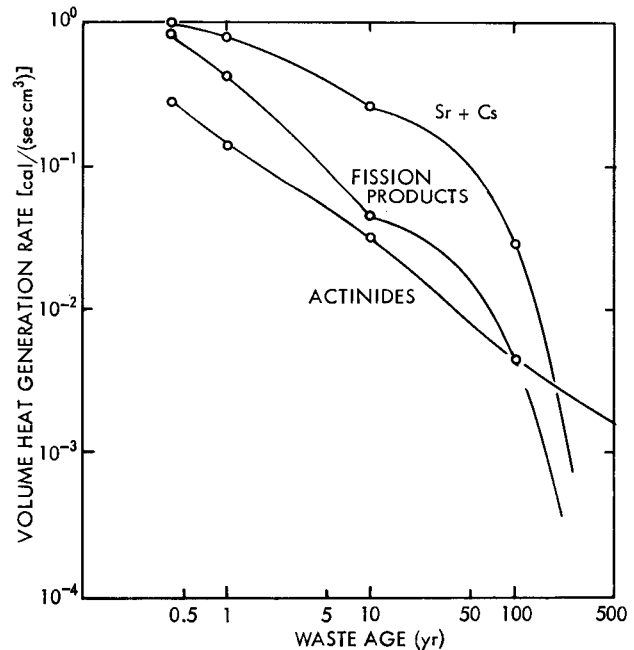


Fig. 5. Volume heat generation rates of pure high-level waste oxides versus age.

generated by a 1000-MW(e) power plant for various volume fractions of radioactive waste oxides in the solidified waste. Calculated densities assume theoretical densities for the waste oxides and 2.5 g/cm³ for the added inert chemicals which make up the balance of the waste volume. The heat generation rates of Table II are reduced linearly by the added inert materials, being proportional to the volume fraction of waste oxides present.

ROCK PROPERTIES

Properties of rock selected for this study are representative of the general classes of basalt and granite types. Values for specific localities will,

TABLE III
Density and Annual Volumes of Waste Generated for Several Volume Fractions of Waste

	Fission Products	Actinides	Sr + Cs
0.15 fraction density (g/cm ³) annual volume (cm ³ /yr) ^a	3.1 9.44 × 10 ⁵	3.8 9.24 × 10 ⁴	2.8 1.48 × 10 ⁵
0.30 fraction density (g/cm ³) annual volume (cm ³ /yr)	3.6 4.72 × 10 ⁵	5.0 4.62 × 10 ⁴	3.1 7.40 × 10 ⁴
0.50 fraction density (g/cm ³) annual volume (cm ³ /yr)	4.4 2.83 × 10 ⁵	6.7 2.77 × 10 ⁴	3.5 4.44 × 10 ⁴

^a1000 MW(e), 35% efficiency, 80% load factor.

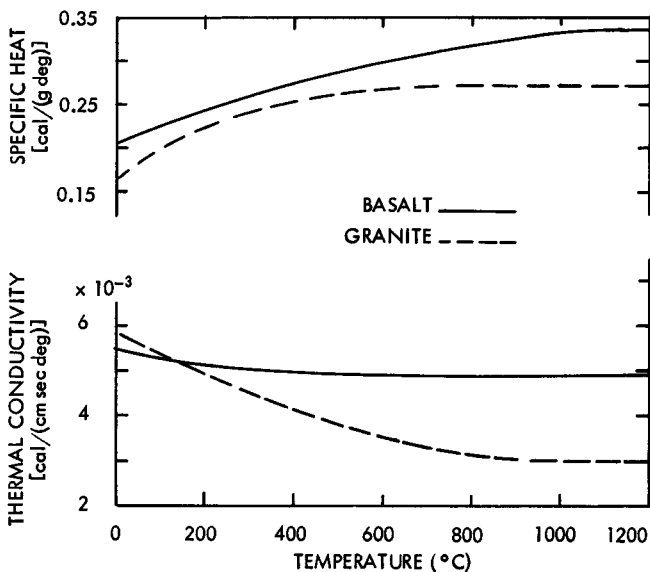


Fig. 6. Specific heat and thermal conductivity of basalt and granite versus temperature.

of course, vary. Density^{9,10} is taken as 2.90 g/cm³ for basalt and 2.65 g/cm³ for granite. Figure 6 shows the variation with temperature for specific heat and thermal conductivity.^{9,10} Both of these properties are assumed to be constant in value above 1000°C. A typical value for the heat of fusion, 100 cal/g, is used for both rock types.

Viscosity is very sensitive to temperature, changing by an order of magnitude with each temperature change of ~150°C. In addition, viscosity varies greatly with variations in composition and water content within a general rock type. Water acts as a fluidizing aid; melting temperature and viscosity decrease as the water content is increased. The viscosity model used in this study is shown in Fig. 7. The curve shown for basalt corresponds to the upper range of viscosities for basalt types as determined by Bottinga and Weill,¹¹ and is double the values reported by Shaw et al.¹² for lava from the Kilauea Volcano, Hawaii. The curve for granite corresponds to data up to 1200°C by Shaw¹³ for 0.6 wt% water, and data by Bottinga and Weill¹¹ between 1300 and 1700°C. The activation energy of viscous flow *E*, in cal/mol, is represented by the slope of the viscosity curve and may be obtained by the simultaneous solution of equations of the form $\eta = A \exp (E/RT)$, evaluated at two points. Values obtained for the

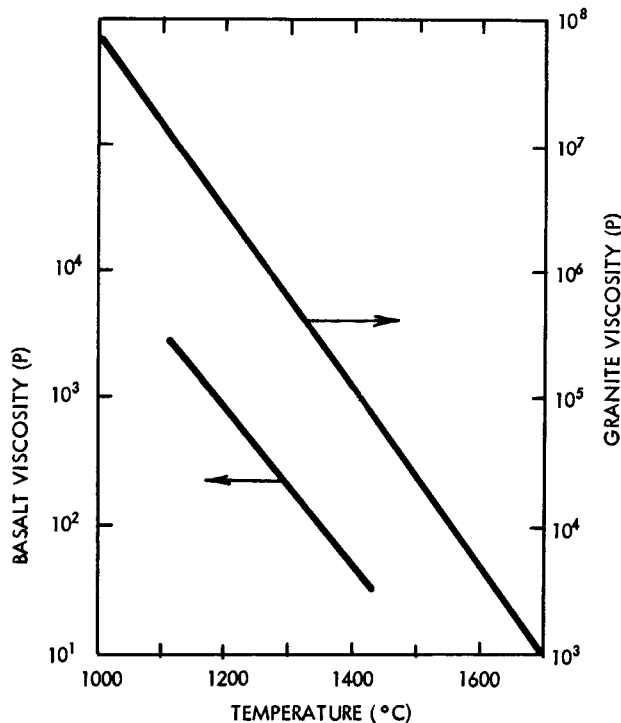


Fig. 7. Viscosity of basalt and granite versus temperature.

viscosity model of Fig. 7 are 68 000 cal/mol for basalt and 100 000 cal/mol for granite. Above temperatures of 1400°C for basalt and 1700°C for granite, viscosity is assumed to level off to a constant minimum value. Temperatures used in this study are therefore limited to levels at or below these values.

Melting occurs over a range of temperatures. For purposes of defining a minimum capsule surface temperature for continued descent, representative melting temperature values of 1150°C for basalt and 950°C for granite are used.

RESULTS OF CALCULATIONS

A series of 42 cases have been analyzed for the three waste categories previously described, volume waste fractions of 0.15, 0.30, and 0.50, and capsule radii of 50 and 100 cm, plus 25 cm for the Sr + Cs category. The container for all cases is assumed to have a wall thickness 3% of the radius and a density of 8 g/cm³. The case descriptions and summaries of computer results are presented in Table IV for basaltic rock and Table V for granitic rock.

The results are easier to interpret if the gen-

eral calculation sequence is first described. For each increment of descent time following release, all properties are reevaluated considering accumulated depth and accumulated age of waste. The specific heat and thermal conductivity of the rock are averaged between the local bulk temperature and the capsule surface temperature. The value of rock viscosity in contact with the capsule is determined and the variation from this value, ahead of the descending capsule, is built into the hydrodynamic equations previously discussed. The sequence summary is as follows:

1. Start with an earliest possible waste age of 0.5 yr and lowest capsule temperature (equal to the rock-melting temperature).

2. Calculate descent velocity by the energy criteria, iterating for the proper velocity-dependent "downward heat fraction."

3. Calculate velocity by the hydrodynamic criteria, using the driving force resulting from differential density.

4. If the latter velocity is not as great as the former, viscosity is too high. Increment capsule temperature upward 10°C and repeat until veloci-

TABLE IV
Calculation Results for Earliest Release Waste Capsule Descent in Basalt Rock

Case No.	Waste		Capsule		Initial Conditions				Descent Time to 1200°C, T_c (yr)	Final Depth		
	Type	Volume Fraction	Radius, a (cm)	Average Density, ρ_c (g/cm ³)	Surface Temp, T_c (°C)	Heat Generation, q''' [cal/(cm ³ sec)]	Waste Age (yr)	Velocity, v (m/day)		Surface Temp, T_c (°C)	Descent Time (yr)	Depth, z (km)
1	Fission Products	0.15	50	3.53	1390	0.107	0.50	2.90	0.75	1150	12	3.9
2		0.30	50	3.98	1400	0.128	1.00	3.53	1.3	1150	41	7.2
3		0.50	50	4.71	1400	0.143	1.50	4.02	1.9	1150	66	12.3
4	Actinides	0.15	100	3.53	1390	0.043	1.50	2.49	1.8	1150	70	8.2
5		0.30	100	3.98	1390	0.047	2.75	2.77	3.1	1150	105	16.2
6		0.50	100	4.71	1390	0.054	4.0	3.23	4.8	1150	140	29.4
7		0.15	50	4.17	1150	0.036	0.50	0.99	0	1150	5.6	2.5
8		0.30	50	5.26	1220	0.073	0.50	2.12	0.05	1150	16	3.9
9		0.50	50	6.81	1320	0.121	0.50	3.54	0.4	1150	31	6.5
10	Sr + Cs	0.15	100	4.17	1310	0.036	0.50	2.20	0.4	1150	37	4.9
11		0.30	100	5.26	1370	0.053	0.75	3.18	1.3	1150	96	10.2
12		0.50	100	6.81	1380	0.060	1.25	3.66	2.5	1150	350	23.3
13		0.15	25	3.25	1250	0.143	0.5	1.76	0.5	1150	30	6.8
14		0.30	25	3.53	1400	0.285	0.5	3.56	2.8	1150	70	19.1
15		0.50	25	3.89	1390	0.303	1.75	3.86	6.3	1150	135	44.4 ^a
16	Sr + Cs	0.15	50	3.25	1400	0.098	1.50	2.60	5.9	1150	100	22.3
17		0.30	50	3.53	1400	0.109	5.0	2.96	25	1150	76	>50 ^a
18		0.50	50	3.89	1400	0.124	12.0	3.41	35	1150	40	>50 ^a
19		0.15	100	3.25	1400	0.039	10.0	2.23	35	1150	110	>50 ^a
20		0.30	100	3.53	1400	0.044	33.0	2.56	35	1150	68	>50 ^a
21		0.50	100	3.89	1400	0.049	49.0	2.90	36	1150	52	>50 ^a

^aPenetrate crust and enter mantle at 35 km.

ties by both criteria are in agreement. If the temperature drives upward past the upper limit, the waste is too "hot." In this case, the initial age of waste is incremented (reduces heat generation by longer decay) and the process is repeated until a descent start within an allowed temperature range is attained.

5. Multiply velocity by the time increment, obtaining the depth increment.

6. Continue incrementing depth until heat generation decays to the local threshold value, at which time further descent is assumed to cease.

7. Repeat for several values of older initial waste ages.

The results summarized in Tables IV and V are for initial ages of 0.5 yr (the earliest time considering reprocessing requirements) or the earliest age for which initial temperature limits (1400°C in basalt, 1700°C in granite) are not exceeded.

Maximum depths attained as a function of the volume fraction of wastes (concentration) are summarized in Fig. 8. Each point is identified by

the case number from Table IV or V, permitting referral to associated information in these tables. As the volume fraction and/or capsule size increases, the attainable depth increases. The high heat output of the Sr + Cs category for the higher concentrations and larger sizes requires unusually long initial aging periods (over 30 yr). The seemingly nontypical trend of the curve with cases 38 and 39 in Fig. 8c is associated with the long aging.

Figure 9 presents a few of the basalt cases, showing depth attained versus time. Space does not permit including more than this sampling. Families of curves show the reduction in depth as the initial waste age increases. The initial surface temperature of the capsule also decreases for older initial age (labeled on the curves). Table IV includes the time required for the temperature to drop from the initial value to 1200°C for the earliest age descent in basalt. Table V includes the corresponding times to drop to 1500°C in granite. The time required for some moderation of temperature and the lowering of initial temperature by increased aging is of interest in the selection of suitable container materials.

TABLE V
Calculation Results for Earliest Release Waste Capsule Descent in Granite Rock

Case No.	Waste		Capsule		Initial Conditions				Descent Time to 1500°C, T_c (yr)	Final Depth		
	Type	Volume Fraction	Radius, a (cm)	Average Density, ρ_c (g/cm ³)	Surface Temp, T_c (°C)	Heat Generation, q''' [cal/(cm ³ sec)]	Waste Age (yr)	Velocity, v (m/day)		Surface Temp, T_c (°C)	Descent Time (yr)	Depth, z (km)
22	Fission Products	0.15	50	3.53	1670	0.043	1.50	1.05	1.5	1080	29	3.9
23		0.30	50	3.98	1700	0.052	2.50	1.30	3.1	1040	60	7.0
24		0.50	50	4.71	1690	0.054	4.0	1.38	4.6	1000	84	10.9
25	Actinides	0.15	100	3.53	1670	0.016	4.0	0.87	3.9	960	86	8.5
26		0.30	100	3.98	1680	0.019	7.0	1.02	20	950	120	13.3
27		0.50	100	4.71	1700	0.022	10.0	1.22	36	950	150	21.4 ^a
28		0.15	50	4.17	1600	0.036	0.50	0.90	0.35	1050	12	2.9
29	0.30	50	5.26	1670	0.053	0.75	1.34	1.2	1030	27	4.4	
30	0.50	50	6.81	1670	0.060	1.25	1.58	2.5	990	56	7.1	
31	Sr + Cs	0.15	100	4.17	1700	0.021	1.00	1.14	2.5	960	64	5.4
32		0.30	100	5.26	1700	0.023	2.50	1.28	6.2	950	240	12.6
33		0.50	100	6.81	1690	0.024	5.0	1.39	9.8	950	500	27.8 ^a
34		0.15	25	3.25	1680	0.107	1.25	1.17	4.0	1180	52	8.0
35	0.30	25	3.53	1690	0.122	4.0	1.36	21	1100	90	16.3 ^a	
36	0.50	25	3.89	1700	0.137	9.0	1.57	37	1000	125	26.8 ^a	
37	Sr + Cs	0.15	50	3.25	1690	0.044	8.0	1.06	32	1020	115	16.8 ^a
38		0.30	50	3.53	1700	0.049	29.0	1.21	37	960	130	20.9 ^a
39		0.50	50	3.89	1700	0.052	47.0	1.30	37	950	135	22.9 ^a
40		0.15	100	3.25	1700	0.017	43.0	0.91	36	950	135	15.9 ^a
41		0.30	100	3.53		q''' too high	>50					
42	0.50	100	3.89		q''' too high	>50						

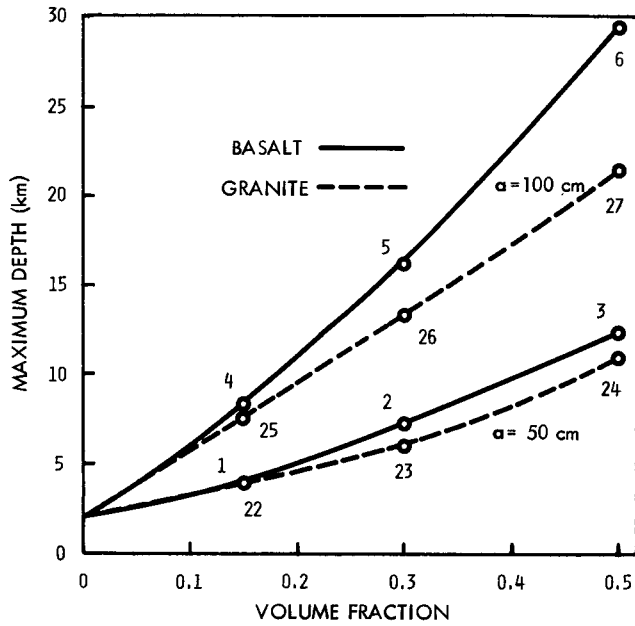
^aPenetrate granite into basalt at 15 to 20 km.

DISCUSSION

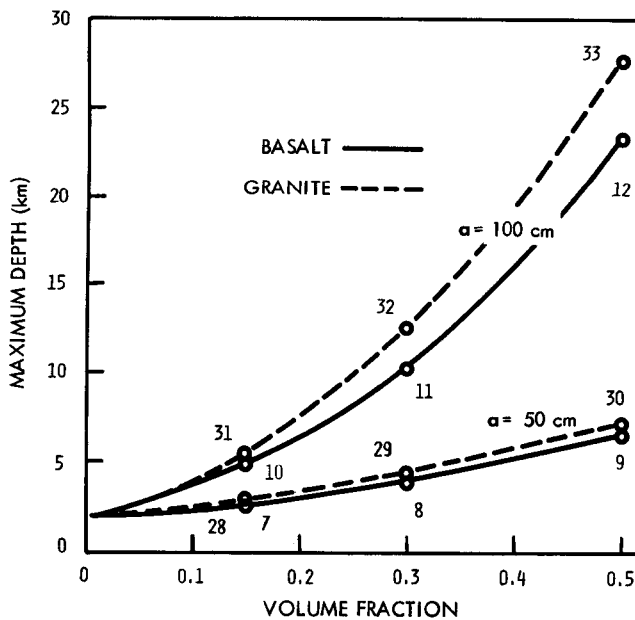
The maximum attainable depths for the various system configurations depend on the capsule remaining as a compact entity during the full descent time. Breakup resulting from container corrosion or erosion permits diffusion and mixing

with the rock melt and terminates travel at shallower depths. Depending on the depth attained prior to such a termination and on depths determined to be required for satisfactory environmental isolation, certain of the systems may provide proper disposal even if breakup does prevent reaching the calculated maximum depths described previously.

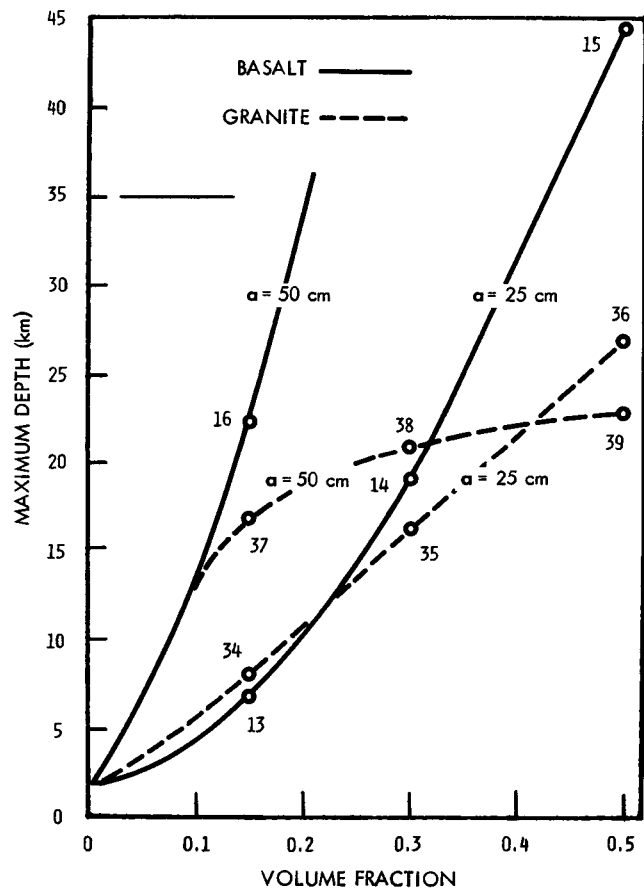
Depths of 10 km or greater are attainable with intact waste capsules of 100-cm radius if the concentration of waste oxides has a volume fraction of at least 20% for fission products and 27% for actinides (Fig. 8). The corresponding initial heat generation rates lie close to 0.05 cal/(sec cm³). This is almost equal to typical current solidified waste product heat generation of 200 W/liter [200 W/liter = 0.0478 cal/(sec cm³)]. However, the latter is probably a lower concentration at a younger age than in the cases presented here. This lower concentration in present product is at least partly due to the addition of inert fillers for the purpose of reducing heat concentrations for



(a) fission products

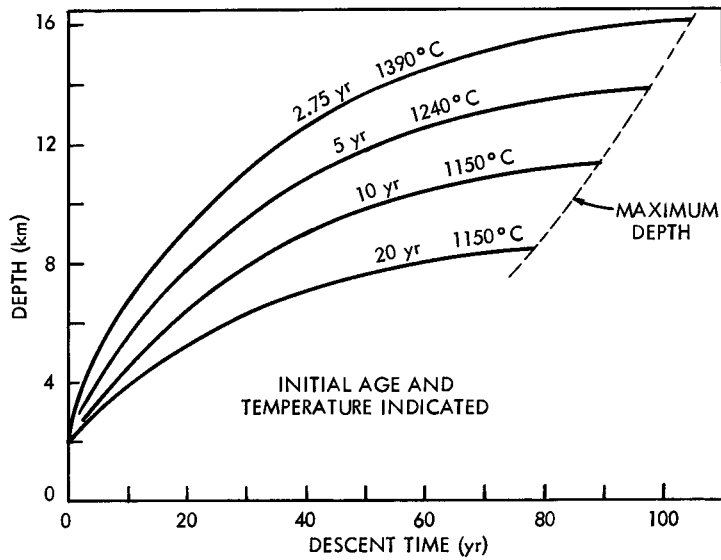


(b) actinides

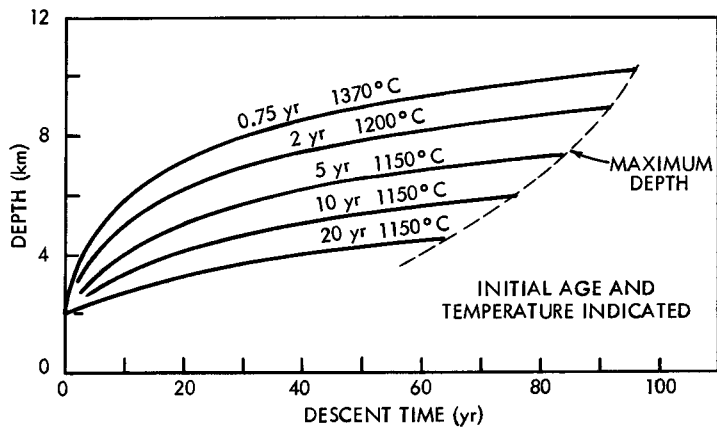


(c) Sr + Cs

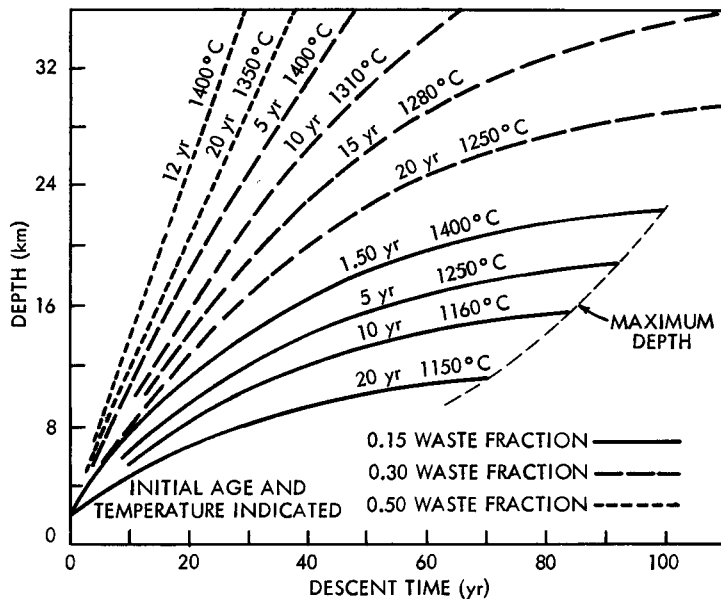
Fig. 8. Maximum depth versus volume fraction of waste. Case numbers are indicated for points.



(a) fission products—
100-cm radius,
0.30 waste fraction
(case 5)



(b) actinides—
100-cm radius,
0.30 waste fraction
(case 11)



(c) Sr + Cs—
50-cm radius,
0.15, 0.30, and 0.50 waste fractions
(cases 16, 17, and 18, respectively)

Fig. 9. Depth attained versus time of descent in basalt.

other concepts of storage. The higher heat generation for Sr + Cs oxides attains the 10-km depth with 20% concentration in the smaller 25-cm radius capsule or only 8% in a 50-cm capsule. It is expected that an objective will be to move the wastes into final disposal with minimum aging. The configurations reported here which indicate long initial aging periods have utility in accommodating wastes accumulated prior to initiation of the disposal site.

Several cases (Table V) indicate penetration through granite into basalt, which can occur at the Conrad discontinuity (a depth of 15 to 20 km). Moderate concentrations of Sr + Cs (Table IV) may result in penetration through the Earth's crust into the mantle, at the Mohorovicic discontinuity (continental depth average, 35 km). The tabulated depths ignore these discontinuities. A two-layer calculation would revise the final depths for the cases affected. Results indicate that the highest Sr + Cs fraction (0.50) in a 50-cm or larger radius capsule descending in basalt reaches a minimum velocity and then begins to accelerate due to movement into hotter rock at a rate that offsets the decay of thermal output. It may also be possible to choose a site in a tectonic subduction zone such that moderate self-burying depths will ensure conveyance into the Earth's interior.

Detailed analysis has been limited to the release of a single capsule into ambient temperature rock. Following descent from the release point, the molten rock wake resolidifies, forming a seal to isolate the waste capsule. Jaeger¹⁴ reports a method for calculating the cooling and solidification of an intrusive rock sheet. By assuming that the time required for solidification of a cylindrical "intrusion" is roughly one-third that of a continuous slab having a semithickness equal to the cylinder radius, and using the method of Jaeger, the times required to solidify the waste capsule wakes are estimated to be as listed in Table VI. The much longer times for granite are due mainly to a cooling temperature interval about three times as great as that for basalt.

During descent, the container serves only as a separator between the waste and molten rock and may be operated at temperatures closer to melt-

ing than would be the case in structural uses. Superalloys may be suitable up to around 1200°C. DiStefano¹⁵ reports corrosion of Haynes alloy No. 25, Hastelloy C, and Type-316 stainless steel by SrO at 1100°C to be a reaction zone up to 10 mils after 10 000 h, with negligibly slow reaction rates after 5000 h. Lithium heat pipes⁷ have been operated with refractory metal tubes at temperatures up to 1330°C with Nb-1%Zr alloys, up to 1430°C with TZM molybdenum alloys, and up to 1830°C with a Ta-10%W alloy. Melter corrosion studies of 15 commercial alloys at 1150°C with a borosilicate waste melt¹⁶ found ten alloys with a corrosion rate of <10 mils/mo. Corronel 230 (35%Cr-65%Ni) and a 20%Cr-45%Ni-5%Mo alloy had rates of <3 mils/mo. A graphite or ceramic outer container with a thin sacrificial metal liner may be considered for wastes having higher densities to offset the 2.25-g/cm³ low-density penalty of graphite, or wastes having heat output high enough to permit replacing a portion with dense ballast. Descent into basalt may be accomplished with a container temperature of ~1200°C, but the high viscosity of granite requires 1500 to 1700°C, a much more severe range.

Successive capsules may be released from the same implantation hole with a delay period between each release to permit resolidification of the rock. Prior to each release, it may be necessary to clean and reshape the bottom of the hole with a drill. A following capsule encounters a column of preheated rock, lowering the heat output required for descent. This permits lower concentrations, older waste, or smaller capsules to be accommodated after a "pilot capsule." Similarly, multiple capsules (Fig. 10a) may be released simultaneously with lower heat output by the trail-

TABLE VI
Days Required to Cool and Resolidify
Waste Capsule Wake

Radius (cm)	Basalt	Granite
25	0.5	6
50	2	24
100	9	95

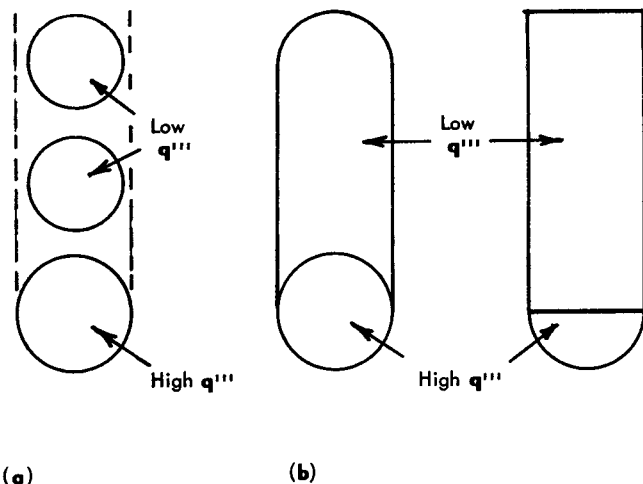


Fig. 10. (a) Multiple release, and (b) double compartment configurations.

ing units. Instead of spherical containers, a double compartment configuration (Fig. 10b) provides high heat output at the penetrator end, a much lower heat output along the sides and trailing end, and a greater driving force for descent.

A single capsule coming to rest as an intact unit becomes enclosed in an envelope of glass as the surrounding layer of melted rock solidifies. An accumulation due to the arrival of successive units may result in further descent by the group. If breakup occurs in the accumulation zone, as illustrated in Fig. 11, the combined heat output results in a rock-melting and mixing mode as in the Plowshare concept of waste disposal.¹

The cooling load during handling and emplacement is plotted in Fig. 12. Disposal on the same site as a fuel reprocessing plant avoids many of the transportation difficulties and may permit casting a waste oxide mixture directly into a disposal container with preinstalled coolant channels (Figs. 13a and b). Where transportation to off-site disposal is necessary, a module configuration may be employed (Figs. 13c and d). Modules, shipped in casks, may be assembled at the disposal site and attached to a temporary cooling system for emplacement. Once the capsule is released for descent, internal module structure or cooling channels are free to melt and mix with the waste contents.

The emplacement hole depth likely may be reduced for some sites to less than the 2 km used here. The LASL Subterrene rock drill⁷ appears

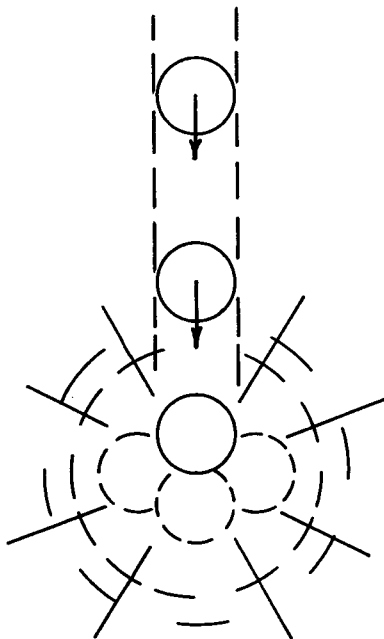


Fig. 11. Accumulation and breakup zone.

to be well suited for making the hole, at substantially less expense than by conventional methods.

The capacity of each waste capsule, in terms of reactor years, using annual volumes for each waste category and concentration from Table III are listed in Table VII. For example, a capsule of 100-cm radius containing a 30% waste fraction may contain the fission-product and actinide wastes from one year of operation of 7.4 power plants.

CONCLUSIONS AND RECOMMENDATIONS

This study indicates that the concept of self-burial of radioactive wastes by rock-melting capsules is feasible. Adequate heat generation is available with moderate waste concentrations for capsules 1 to 2 meters in diameter. Maximum depths >10 km are attainable on energy and hydrodynamic bases; the maximum depth increases with waste concentration and capsule size. A solid rock seal forms above the descending capsule to permanently isolate the waste from

TABLE VII
Capacity of Waste Capsule in Reactor Years
[1000-MW(e) Plants]

Capsule Radius (cm)	Waste Fraction	Capacity			
		Fission Products	Actinides	Total Waste	Sr + Cs
50	0.15	0.5	4.8	0.5	3.0
	0.30	1.0	9.7	0.9	6.0
	0.50	1.6	16.2	1.5	10.1
100	0.15	4.0	41.4	3.7	25.8
	0.30	8.1	82.8	7.4	51.7
	0.50	13.5	138.0	12.3	86.2

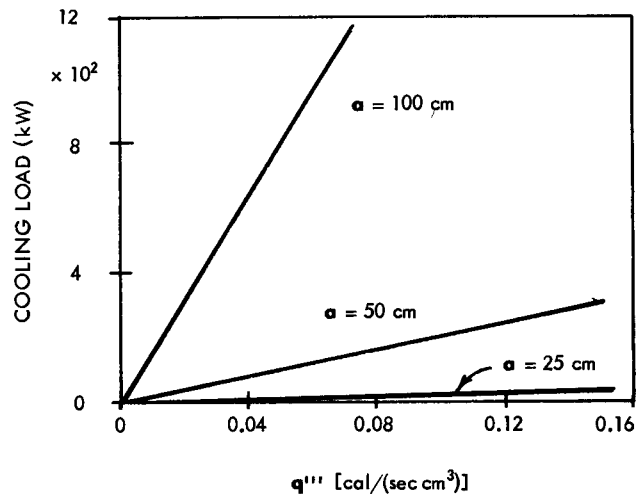


Fig. 12. Initial cooling load versus heat output of waste.

the environment. The surface land at the disposal site may be returned to other uses following a short surveillance period. Each hole may be used for the release of several capsules per year. Release of capsules at 3-wk intervals, with a 100-cm radius and 0.30 waste fraction, would allow a single disposal hole in basalt to accommodate the total predicted U.S. nuclear power industry in 1980: 130 000 MW(e). Multiple release holes at a disposal site can utilize smaller capsules and/or lower concentrations.

Recommendations for further work on the rock-melting-capsule concept to provide for a demonstration system are as follows:

1. *High-level waste solidification.* Investigate maximization of waste oxide concentration and density of the solid product. The use of higher density additives should be examined. Study chemical alterations that may be needed for melt stability and for the reduction of metal corrosion by high-temperature melts.

2. *Container materials.* Investigate high-temperature corrosion and erosion in contact with waste oxide melts and molten rock for refractory metals, ceramics, and composites.

3. *Site survey.* Determine suitable locations for demonstration of the concept and determine the release depths and descent depths required to ensure environmental protection. Include consideration of tectonic subduction zones.

4. *High-temperature rock properties.* Extend investigations of basaltic and granitic rock properties at high temperatures.

In addition, follow-on system design studies should evaluate risks, assembly configurations, transportation and field-handling methods, and cooling systems.

REFERENCES

1. J. J. COHEN, A. E. LEWIS, and R. L. BRAUN, "In-Situ Incorporation of Nuclear Waste in Deep Molten Silicate Rock," *Nucl. Technol.*, **14**, 76 (1972).
 2. J. DONEA, S. GIULIANI, and L. KESTEMONT, "Self-Burial Process of Containers Filled with Highly Active Wastes (Preliminary Report)," EUR-4903f, Commission of the European Communities (1972); also, Euro-Spectra, XI:102 (1972).

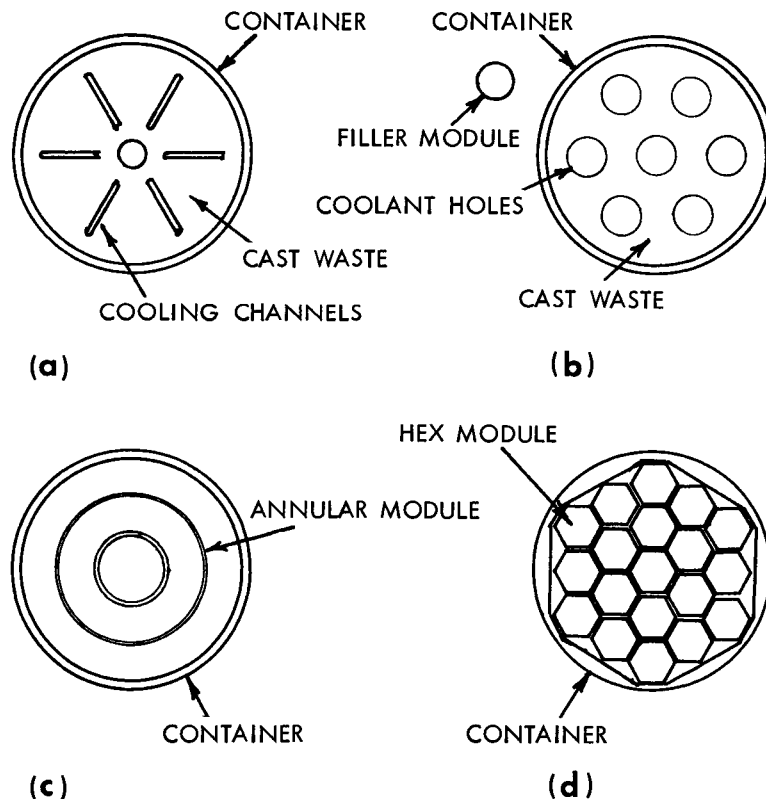


Fig. 13. Provisions for initial cooling of capsule.

3. C. R. EASTON, "Conduction from a Finite-Size Moving Heat Source Applied to Radioisotope Capsule Self-Burial," NBS Special Publication 302, p. 209, National Bureau of Standards (1968).
4. R. E. ISAACSON and L. E. BROWNELL, "Ultimate Storage of Radioactive Wastes in Terrestrial Environments," ARH-SA-126, Atlantic Richfield Hanford (1972).
5. P. J. SCHNEIDER, *Temperature Response Charts*, p. 39, John Wiley and Sons, Inc., New York (1963).
6. D. E. ARMSTRONG, J. S. COLEMAN, B. B. McINTEER, R. M. POTTER, and E. S. ROBINSON, "Rock Melting as a Drilling Technique," LA-3243, Los Alamos Scientific Laboratory (1970).
7. E. S. ROBINSON, R. M. POTTER, B. B. McINTEER, J. C. ROWLEY, D. E. ARMSTRONG, R. L. MILLS, and M. C. SMITH (Ed.), "A Preliminary Study of the Nuclear Subterrene," LA-4547, Los Alamos Scientific Laboratory (1971).
8. "Siting of Fuel Reprocessing Plants and Waste Management Facilities," ORNL-4451, Oak Ridge National Laboratory (1970).
9. S. P. CLARK, Jr., Ed., *Handbook of Physical Constants*, Memoir 97, The Geological Society of America (1966).
10. F. BIRCH, J. F. SCHAIRER, and H. C. SPICER, Eds., *Handbook of Physical Constants*, Special Papers No. 36, The Geological Society of America (1942).
11. Y. BOTTINGA and D. F. WEILL, "The Viscosity of Magmatic Silicate Liquids: A Model for Calculation," *Am. J. Sci.*, **272**, 438 (1972).
12. H. R. SHAW, T. L. WRIGHT, D. L. PECK, and R. OKAMURA, "The Viscosity of Basaltic Magma: An Analysis of Field Measurements in Makaopuhi Lava Lake, Hawaii," *Am. J. Sci.*, **266**, 225 (1968).
13. H. R. SHAW, "Comments on Viscosity, Crystal Settling, and Convection in Granitic Magmas," *Am. J. Sci.*, **263**, 120 (1965).
14. J. C. JAEGER, "The Temperature in the Neighborhood of A Cooling Intrusive Sheet," *Am. J. Sci.*, **253**, 306 (1957).
15. J. R. DiSTEFANO, "Compatibility of Strontium Compounds with Superalloys at 900 and 1100°C," *Nucl. Technol.*, **17**, 127 (1973).
16. A. M. PLATT, *Research and Development Activities: Waste Fixation Program, Quarterly Report, July-November 1972*, BNWL-1699, Battelle-Northwest (1972).